SCA2003-39: INVESTIGATION OF LIQUID IMBIBITION MECHANISMS USING NMR

Minghua Ding[1,2] and Apostolos Kantzas[1,2]
1: Department of Chemical and Petroleum Engineering, University of Calgary
2: TIPM Laboratory

This paper was prepared for presentation at the International Symposium of the Society of Core Analysts held in Pau, France, 21-24 September 2003

ABSTRACT

In this study, on-line NMR relaxometry is introduced as a method for monitoring co-current imbibition. A group of plugs from a Western Canada sandstone reservoir was selected and a series of primary and spontaneous imbibition tests were run for both water and oil at the same conditions. Air was the "non-wetting" phase. NMR was used to measure the amount of water or oil imbibed in the cores and to determine the gas saturation during the experiment. The residual gas saturation results from water imbibition tests were compared with the ones obtained from oil imbibition tests. The imbibition rates and the correlations of residual gas saturation with initial imbibition rates for both types of imbibition tests were also investigated. Through interpretation of the NMR spectra, bound water or oil $T_{2cutoff}$ values were determined. The distributions of water and oil in different pore sizes were compared. The initial imbibition rate at different pore sizes was measured. Finally, a literature model was used to check our experimental data.

Preliminary results indicate that oil and water do not imbibe in the same way. The NMR spectra indicate that there is no substantial oil penetration of the small pores within the experimental period of two months. Comparing current results with previous results in soils, it becomes evident that spontaneous imbibition with on-line NMR measurements can become a tool for wettability assessment.

Other applications of the on-line NMR measurements deal with the determination of residual gas saturation and gas recovery from gas reservoirs.

INTRODUCTION

Wettability is one of most important reservoir parameters. It is defined as "the tendency of one fluid to spread on or adhere to a solid surface in the presence of other immiscible fluids. For an oil-water system, different recovery mechanisms will be applied for different wettability condition. For a gas –liquid system, gas is usually considered the non-wetting phase and liquid is considered the wetting phase. Non-wetting phase displacing wetting phase is called drainage and wetting phase displacing non-wetting phase is called "imbibition". When no external forces apply on a system, the imbibition is called "spontaneous" or "free" imbibition. When there is an external force applied on the system, the imbibition is called forced imbibition or controlled imbibition depending on the external forced was applied on the inlet end or outlet end of the sample. According to the capillary theory of imbibition [1], when the wetting phase starts to enter

the porous media, it will occupy the porous media from the smallest pore and form thin films over all the rock surfaces. Many researchers [1-4] described how imbibition works in a displacement experiment through simple capillary systems such as capillary tubes and network micromodels.

Chatzis [1] described several fundamental aspects of the invasion of pore space by a wetting phase under free imbibition conditions. The experimental work for studying free imbibition aspects was performed in glass micromodels. He found out that the Washburn Equation [5], which was used to describe the advance of the meniscus of a wetting phase imbibing into a horizontal capillary tube with time, couldn't be used to predict the depth of infiltration with time when significant entrapment of gas occurred. He concluded that the spontaneous imbibition of a wetting liquid along the edges of pores was a very important flow mechanism that facilitated the mass transport ahead of the "apparent" imbibition front.

Lenormand et al. [2] researched the mechanism of displacement of one fluid by another in a network of capillary ducts. The experiments were set up in a single duct firstly and then in an intersection. The basic mechanisms were developed based on 'piston-type' motion and 'snap-off'. They figured out that capillary pressure for 'piston like' motion is always greater than that for the capillary pressure for 'snap-off' and 'snap-off' occurs only when 'piston-type' motion is not possible for topological reasons. They also showed that the Laplace Law linking the capillary pressure to the interface curvature could describe their observations.

Li and Wardlaw [3, 4] studied the mechanisms of nonwetting phase trapping during slow rate imbibition and critical pore-throat size of snap-off under different wettability. The experiments were performed in transparent-glass micromodels. Nonwetting phase trapping in porous media can be caused by snap-off or break-off. The snap-off involved selloidal menisci and could occur within throats, within pores or at the junction region of pores and throats, while break-off referred to rupture during piston type advance of a convex interface which contacted opposing pore walls. The aspect ratio (pore to throat ratio) for snap-off in throats is 1.5 when advancing contact angle is zero and increased slightly to 1.75, when the advancing angle is 55°. When advancing angle is greater than 70°, the snap-off in throats will never happen.

Kantzas et al. [6] developed a kinetic model of imbibition in soils. A series of tests were conducted in soil samples, both contaminated and clean. The imbibition tests were done in a counter current fashion with controlled water rates and measured using low field NMR relaxometry. It was found that the NMR spectra could be resolved into peaks corresponding to different pore sizes. The intensities and sizes of peaks changed as a function of time and the NMR could monitor the distribution of water in the porous media. Through analysis of water migration, a kinetic model of imbibition was formulated, with constants that described the water uptake in the different pore sizes.

Li and Horne [7] developed an equation to describe the relationship between the imbibition rate and gas recovery based on the assumption of a piston-like imbibition

flow. In their equation, the imbibition rate should be in a linear relation with the reciprocal of gas recovery. They performed co-current water imbibition tests in a balance using a glass bead pack and a Berea sandstone plug. The results from their experiments fit the equations they developed.

The Li and Horne equation is:

$$Q_w = \frac{dN_{wt}}{dt} = a\frac{1}{R} - b \qquad (1)$$

Where:

$$a = \frac{Ak_w(S_{wf} - S_{wi})}{m_w L} P_c, \qquad (2)$$

$$b = \frac{Ak_w}{m_w}\Delta rg \qquad (3)$$

$$R = \frac{N_{wt}}{V_p} \qquad (4)$$

Where L and V_p are the core length and pore volume of the core sample, R is gas recovery, A is cross section area of core, K_w is effective water permeability, S_{wf} is water saturation behind water front, S_{wi} is the initial water saturation, P_c is capillary pressure, m_w is water's viscosity, a is capillary pressure coefficient and b is gravity coefficient respectively.

Chatzis and Morrow [8] performed co-current imbibition tests by building relatively high residual oil saturation from forced imbibition using a small external force gradient, and then gradually increasing the pressure gradient until there was some residual oil production. They found that the critical capillary number for mobilizing the residual oil in porous media is 10^{-5}. Dong et al. [9] developed a 'complete' capillary number by considering the length L and radius R of the capillary tube. The complete capillary number was further used to characterize saturation profile histories measured in imbibition and in waterfloods. When the 'complete' capillary number is much less than 1, the imbibition is controlled by capillary force and the saturation rises uniformly along the entire length of the plug. When the 'complete' capillary number is much greater than 1, the imbibition is controlled by viscous force and there is a step change in saturation from the connate water to the residual oil value, advancing as a piston.

In the present study, the behavior of water and oil spontaneous imbibition into dry plugs from spontaneous imbibition tests will be addressed. The imbibition rate, liquid saturation distribution in different pore sizes, $T_{2cutoff}$ and residual gas saturation were investigated. In three plugs, water imbibition followed oil imbibition tests. Some results and discussions of these plugs were also included in this paper [11].

Porosity and pore size information can be estimated from NMR measurements [10]. The NMR estimation of producible porosity is called the free-fluid index. The estimate of free fluid index is considered the movable fluids that reside in large pores, whereas the bound fluids reside in small pores. Since T_2 value can be related to the pore sizes, a T_2 value can be selected below which the corresponding fluids are expected to reside in small pores and above which the corresponding fluids are expected to reside in larger pores, this T_2 value is called $T_{2cutoff}$. Through the partitioning of the $T_{2cutoff}$ distribution, the pore volume can be divided into free fluid index and bound-fluid porosity.

When the rock is liquid-wet, there is a tendency for liquid to occupy the small pores and to contact the majority of the rock surface. So for a liquid-wet system, when liquid imbibition happens, liquid is imbibed into the smaller pores first and then occupies the large pores. In NMR spectra, this is represented by a fast relaxing peak and slow relaxing peak, which corresponds to the small pores and large pores respectively. The corresponding value of liquid saturation can be determined from NMR imbibition tests by monitoring the amplitude and relaxation time in the fast peak and slow peak respectively.

EXPERIMENTAL

Preparation of samples

Five sandstone plugs selected from Western Canadian were reservoirs used to do co-current water and oil imbibition while being monitored in NMR. Water imbibition tests followed a primary oil imbibition tests in three plugs (Plugs #A, #B and #D). The plugs are approximately 3.8cm in diameter and approximately 5cm in length. At the beginning of the experimental program and between each procedure, each plug was cleaned in a Dean Stark apparatus and then dried in an oven. Before the experiments, the plugs were dried to 100% air saturation. All the experiments were preformed under atmospheric pressure. There was no specific effort to saturate the liquid with gas [11].

The pore volume was measured using the Archimedes principle. The plugs were saturated in synthetic formation brine. The pore volume was then calculated by measuring the weight change of the core and the weight and volume of the liquid that the core displaces when immersed in synthetic formation brine. Subsequently porosity was calculated. The density of the brine was measured by using a Brookfield densitometer. Measurements of air permeability were performed prior to the spontaneous imbibition tests (see Table 1). The density and viscosity of brine is 1.0225 g/cm^3 and 1 mPa.s respectively. The oil used for imbibition tests was a mixture of soltrol and paraffin mineral oil, for which the density and viscosity are 0.8114 g/cm^3 and 6.6 mPa.s respectively. This experimental procedure thus emulates spontaneous imbibition only.

Imbibition experiments

The experiments for both water and oil imbibition were performed as co-current spontaneous primary imbibition tests. Primary imbibition is defined as imbibition started without initial water saturation. Co-current imbibition is defined when only one face of the plug is in contact with liquid. The co-current imbibition test was performed inside a flow-through NMR relaxometer (Figure 1). The core was placed in a core holder made

out of Teflon. The end face of the core was connected to a piston. By removing the piston, water was allowed to imbibe in the core. Before the test, an NMR standard was measured to ensure that the accuracy of the machine is acceptable (±2%). Then the dry plug was measured at the beginning as a basis of each experiment. After liquid started imbibing, the amplitude and relaxation profile change as a function of time were recorded automatically. Furthermore the weight of liquid imbibed was calculated. The amount of liquid imbibed into small pores and large pores was interpreted from the observed NMR spectra during each imbibition experiment. Mass balance was used to verify the final gas saturation.

RESULTS AND DISCUSSION

Gas saturation

The residual gas saturation results from both water and oil co-current imbibition tests for the five plugs used in this work are presented in Figure 2. The values of residual gas saturation from both procedures are close for most plugs (Plug A is an exception). Figures 3-7 show the gas saturation change with time for the five plugs during both water and oil imbibition tests. Gas saturation change with time was calculated from the amplitude change of water imbibed into the plug with time. At each time step the amount of imbibed water or oil is calculated from the NMR spectra. The total amplitude of the imbibed water (A_T) is normalized to the amplitude index (AI) for the specific water sample. AI is defined as the amplitude per unit mass in a given liquid sample. The ratio A_T/AI is then equal to the imbibed mass. This mass is then divided by the density of the water and it is normalized against the pore volume of the sample to provide the liquid saturation (S_L). The saturation of gas, is defined as $S_g=1-S_L$.

$T_{2cutoff}$

In conventional NMR analysis, the spectrum of a saturated sample contains two basic components, the flowing component or free fluid index (FFI) and the bulk volume irreducible (BVI), which is total porosity minus free fluid index [10]. The separation of FFI and BVI is the so-called $T_{2cutoff}$ and it is obtained through the comparison of the NMR spectra at $S_w=1$ and $S_w=S_{wir}$. In this work the primary imbibition test is used to determine the $T_{2cutoff}$. As imbibition commences, spectra appear to increase in amplitude as a function of time. An example is shown in Figures 8 and 9 for Plug D during water and oil imbibition tests. Similar curves were obtained for the other four plugs. The location of each peak in a given spectrum does not seem to change. The peaks at faster relaxation times in the spectra stand for the water or oil imbibed in smaller pores. The peaks at slower relaxation times in the spectra represent the water or oil imbibed in the larger pores. The $T_{2cutoff}$ values were determined by using the relaxation time between small peaks and large peaks as shown in the graphs. Even if the $T_{2cutoff}$ was used to separate FFI and BVI, the values are not the same for water and oil imbibition tests. For plug D, the $T_{2cutoff}$ for the spectra is determined to be 56 ms for water imbibition (Figure 8) whereas it is 25 ms for oil imbibition (Figure 9). The shape and location of peaks are also different. The large peak for water imbibition test is wider and shorter and T_{2max}=200 ms (Figure 8) while it is narrower and taller for oil imbibition test and T_{2max}=250 ms (Figure 9). Viscosity affects the relaxation time and diffusion coefficient

of a liquid; therefore the viscosities of water and oil may cause this difference. However, the viscosities of oil (6.2 mPas) and water (1 mPas) are not very different. The differences in spectra can be also attributed to differences in the to surface relaxivity or to immersion related uncertainties [10]. These issues were not addressed in this paper.

Liquid distribution

By taking into account the area under the smaller peaks and the area under the larger peaks, the amount of water or oil imbibed in the smaller pores and larger pores respectively can be calculated. Since the spectra change with experimental time, the liquid distribution with time at different pore sizes can be calculated. Figures 10-14 are results of water and oil distribution in different pore sizes of all plugs. The liquid distribution in different pore sizes varies significantly for different samples.

The data shown in Figures 10 to 14 can be of great importance in accessing the imbibition capacity (therefore the wettability) of a given porous rock. For example, in Figure 10 for plug A, it can be seen that the imbibition in smaller pores is completed in the first 5 minutes of the test while imbibition in the larger pores continues for over 20 minutes for the water imbibition test. On the contrary, in Figure 11 for plug B, imbibition in smaller pores continues for over 200 minutes and imbibition in the larger pores continues for over 2000 minutes for water imbibition test. The imbibition times for the remaining three plugs were somewhere in between (Figures 12-14). But there is another difference between oil imbibition tests and water imbibition tests. For each plug, there is only a very small amount of oil entering the smaller pores immediately, the bulk of imbibition occurring in large pores (Figures 10-14). This can also be observed from Figure 9. The oil imbibition in larger pores is different in different plugs. It continues 100 minutes in plug A, 500 minutes for plug D and over 1000 minutes in the other plugs.

The differences between water and oil imbibition may be caused by the differences in wettability of water and oil with respect to the solid surface. The results of plugs A, B and D, which were selected to perform water imbibition tests following oil imbibition tests, showed different evidence. For plug A, the experiment indicated there was no water imbibed into the porous media after one week. For plug B, when the water imbibition test was performed after the oil imbibition test, some water imbibed into the porous media from both smaller pores and large pores and displaced some amount of oil out; there was no additional gas recovered. For Plug D, some water imbibed into the porous media from both smaller pores and large pores and displaced some amount of oil out; some residual gas came out as well. Therefore much lower residual gas saturation resulted. The three plugs showed three different situations. Plug A can be considered more oil wet than water wet, and Plug B and D have mixed wettability to water and oil.

Imbibition rate

Even though the residual gas saturation results for the five plugs are very close, the shape of curve of gas saturation changing with time for between oil and water is different for all five plugs (Figures 3-7). The curves for plugs A and D have similar shapes for both water and oil imbibing. The remaining three plugs have different but similar shapes. For plugs A and D, water imbibition at the beginning is much faster than oil and then both

curves come together. For the other three plugs, the imbibition rate for water and oil at beginning are not very different. The reason for this may be that plugs A and D have larger permeability and the other three plugs have smaller permeability values. If we define the initial imbibition rate indicator as the slope of gas saturation as a function of experimental time on the semi-log coordinate (Figures 3-7) before the first plateau, this parameter for both water imbibition and oil imbibition is strongly affected by plug permeability (Figure 15).

The Li and Horne [7] method was also used to analyze the imbibition experiment results. Contrary to the method described in Li and Horne, the flow rate ($Q_w = dN_{wt}/dt$) is calculated through fitting the experimental data to simple analytical expressions ($N_{wt}(t)$). These expressions vary both in form and coefficient values for different sections of the imbibition experiment and for different plugs. However, these expressions can provide simple analytical formulas for the rate of imbibition as a function of time. The analytical expressions were then used to obtain plots against the inverse recovery ($1/R$). These plots are shown in Figure 16 for water imbibition tests and Figure 17 for oil imbibition tests. The data follows the trends expected by Li and Horne.

From the Li and Horne's model, a is the coefficient of capillary pressure and b is the coefficient of gravity. Figure 18 presents the correlation of coefficient between water and oil imbibition. It indicates that the ratio of capillary pressure applied for water imbibition to oil imbibition is similar to the ratio of gravity applied to both systems. In other words, the Bond number for both systems is similar.

CONCLUSIONS

Several conclusions could be drawn from this study:

- On-line NMR relaxometry has been successfully used to monitor co-current imbibition tests and determine residual gas saturation, $T_{2cutoff}$ points, liquid distribution in different pore sizes and the initial imbibition rate indicator in different pore sizes.
- The residual gas saturation from water imbibition is very close to the values from corresponding oil imbibition tests for the plugs.
- The initial imbibition rate indicator in strongly affected by air permeability. The correlation between imbibition rate and the reciprocal of gas recovery from both water and oil imbibition tests fit the Li and Horne's Model.

NOMENCLATURE

a	coefficient presenting capillary pressure	b	coefficient presenting gravity
A	cross-section area	A_T	total NMR amplitude
AI	amplitude index	g	gravity constant
k_w	effective water permeability at S_{wf}	P_c	capillary pressure at S_{wf}
K	absolute air permeability	L	length of core sample
N_{wt}	volume of water imbibed into the core	Q_w	water imbibition rate
R	gas recovery by water imbibition	S_g	gas saturation
S_{gr}	residual gas saturation	S_{wi}	irreducible water saturation
S_{wf}	water saturation behind the water front	S_L	Liquid saturation
T_2	transverse relaxation time	t	imbibition time
V_p	pore Volume	Dr	density difference between gas and water
m_w	water viscosity	PV	pore volume

REFERENCES

1. Chatzis, I., "Pore Level Aspects of Liquid Infiltration in 'Dry' Porous Media", AFS Filtration and Separation Society Conference, Nashville, Tennessee, April 23-26, 1995.
2. Lenormand, R., Zarcone, C. and Sarr, A., "Mechanisms of Displacement of one Fluid by Another in a Network of Capillary Ducts", *J. Fluid Mech*. **135**, pp. 337-353, 1983.
3. Li, Y. and Wardlaw, N. C., "Mechanisms of Nonwetting Phase Trapping during Imbibition at Slow Rates", *J. Col. Interf. Sci.*, **109**(2), pp. 473-486, 1986.
4. Li, Y. and Wardlaw, N. C., "The Influence of Wettability and Critical Pore-Throat Size Ratio on Snap-Off"", *J. Col. Interf. Sci.*, **109**(2), pp. 461-472, 1986.
5. Washburn, E., W., *Proc. Nat. Acad. Sci*., **7**, 115, 1921.
6. Kantzas, A., Todoruk, T., Manalo, F. and Langford, C.H., "A Kinetic Theory of Imbibition in Porous Media", Paper SCA 2001-30, presented at the 2001 International Symposium of the Society of Core Analysts, held in Edinburgh, UK, September 17-20, 2001.
7. Li, K. and Horne, R. N., "Characterization of Spontaneous Water Imbibition into Gas-Saturated Rocks", SPE 62552, *SPE Journal*, **4**(6), pp. 375-384, 2001.
8. Chatzis, I. and Morrow, N. R., "Correlation of Capillary Number Relationships for Sandstone", *Pet. Trans. AIME*, **277**, pp. 555-562, 1984.
9. Dong, M., Dullien, F. and Zhou, J., "Characterization of Waterflood Saturation Profile Histories by the 'Complete' Capillary number", *Transport in Porous Media* **31**, pp. 213-237, 1998.
10. Coates, G., Xiao, L., and Prammer, M., "NMR Logging Principle & Applications, Halliburton Energy Services", USA, 1999.
11. Ding, M. and Kantzas, A., "Evaluation of gas saturation during water imbibition experiments", CIPC Paper 2003-021 Canadian International Petroleum Conference, Calgary, Alberta Canada June 10-12, 2003.

TABLE 1: Routine core properties

Plug I.D	Length (cm)	Diameter (cm)	K_{air} (mD)	K_{brine} (mD)	Porosity (%)
A	5.065	3.84	608.5	93.48	15.89
B	5.065	3.87	138.3	14.216	8.97
C	5.01	3.86	45.57	12.47	5.36
D	5.07	3.84	378.17	85.74	9.79
E	5	3.86	114.5	25.65	7.09

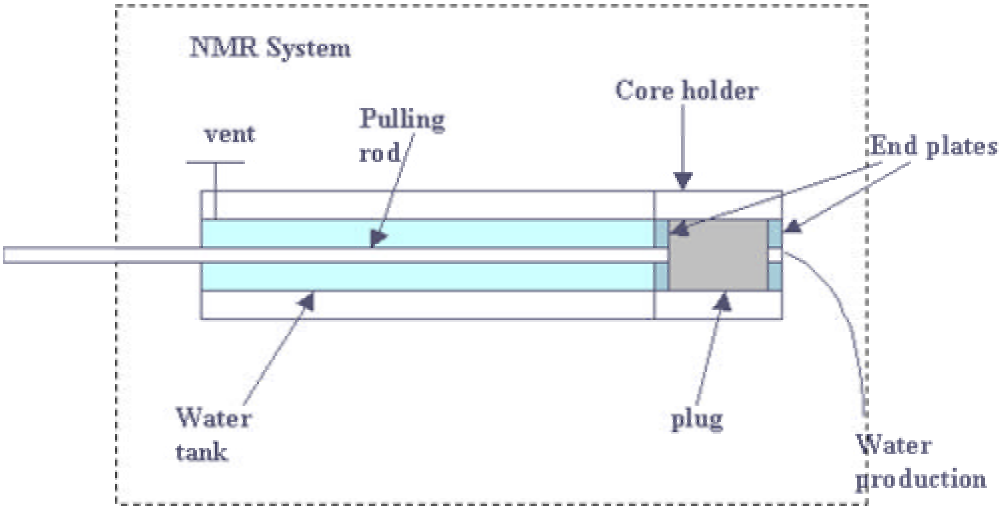

Figure 1: Co-current imbibition in NMR system

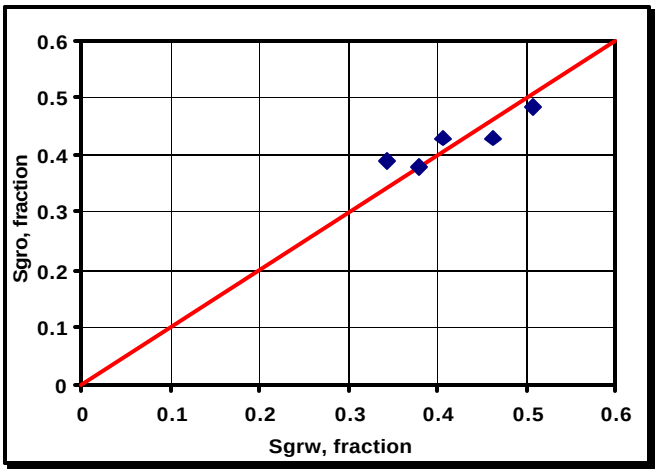

Figure 2: Residual gas saturation results from water and oil imbibition tests

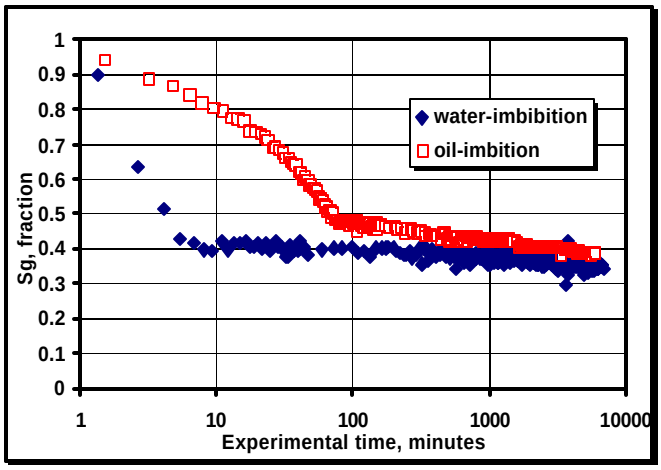

Figure 3: Gas saturation as a function of experiment time of plug A

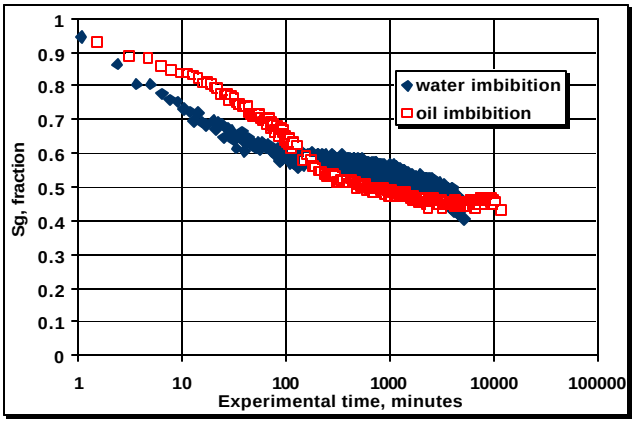

Figure 4: Gas saturation as a function of experiment time of plug B

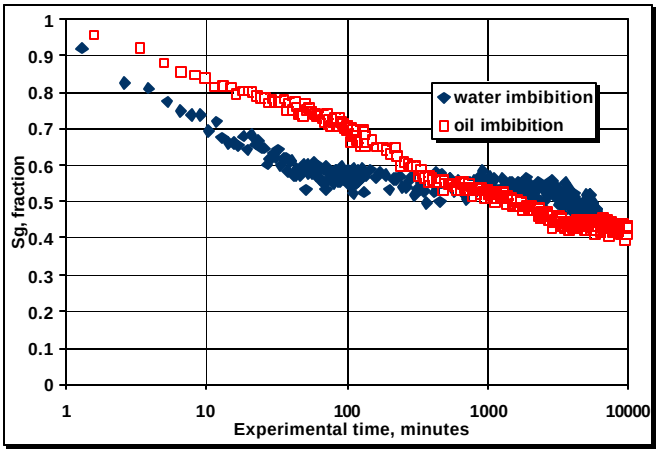

Figure 5: Gas saturation as a function of experiment time of plug C

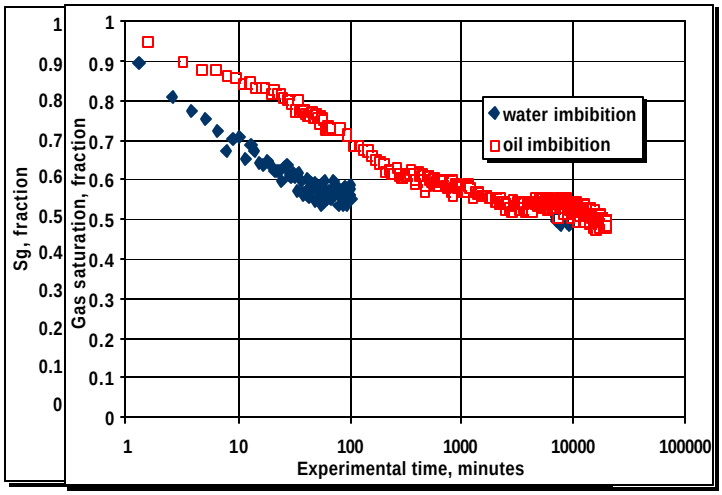

Figure 6: Gas saturation as a function of experiment time of plug D

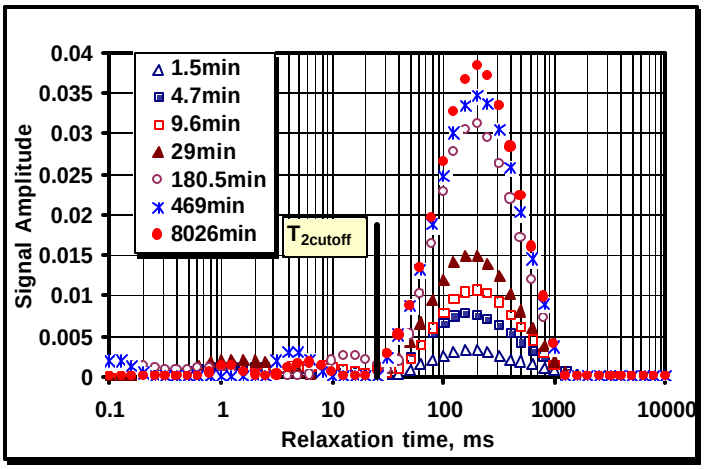

Figure 7: Gas saturation as a function of experiment time of plug E

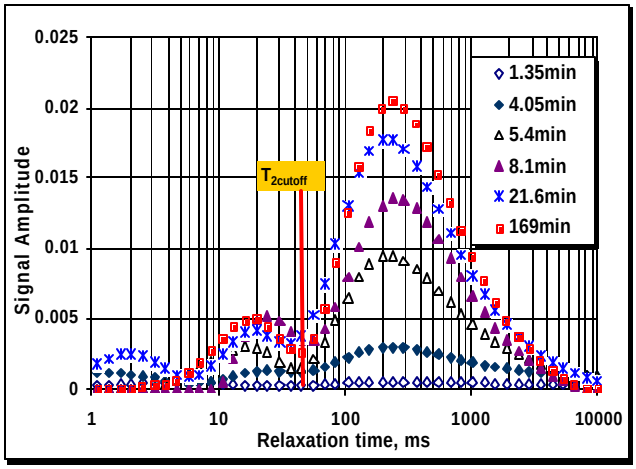

Figure 8: NMR Spectra of water imbibition test of plug D

Figure 9: NMR Spectra of oil imbibition test of plug D

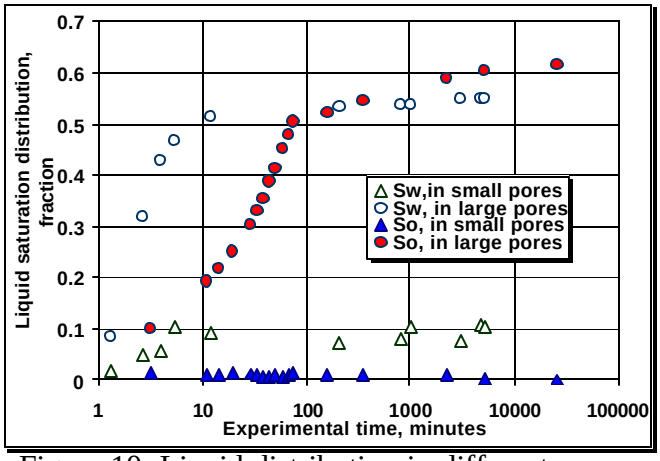

Figure 10: Liquid distribution in different pore sizes of plug A

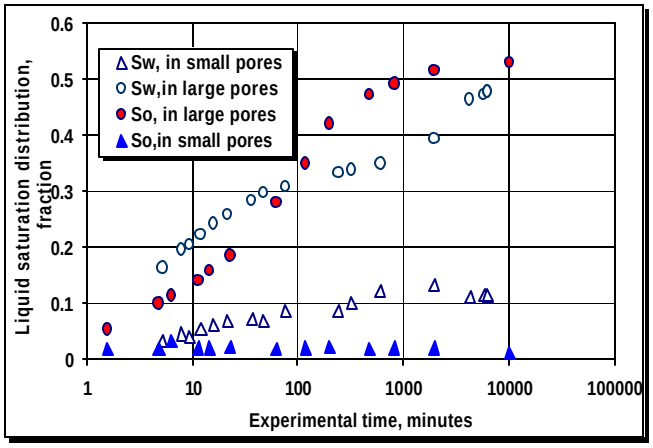

Figure 11: Liquid distribution in different pore sizes of plug B

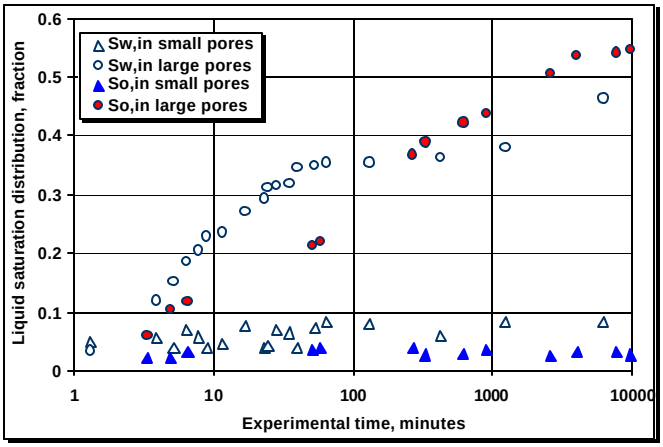

Figure 12: Liquid distribution in different pore sizes of plug C

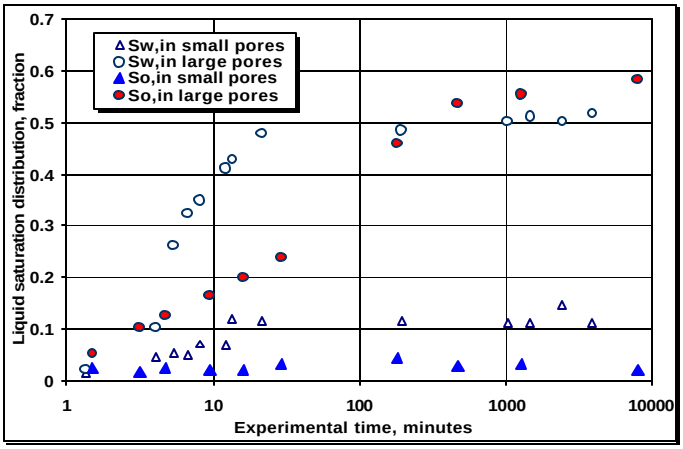

Figure 13: Liquid distribution in different pore sizes of plug D

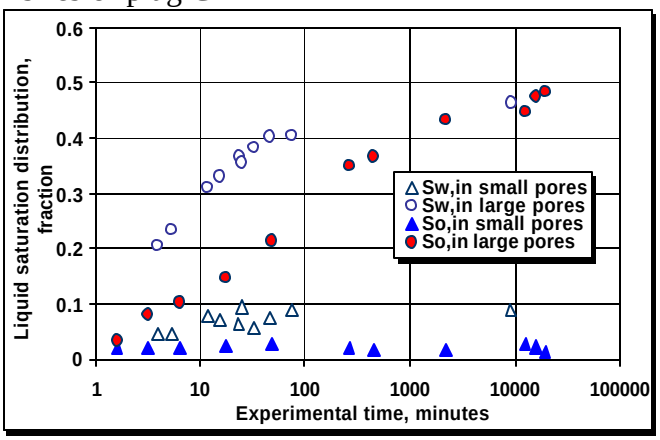

Figure 14: Liquid distribution in different pore sizes of plug E

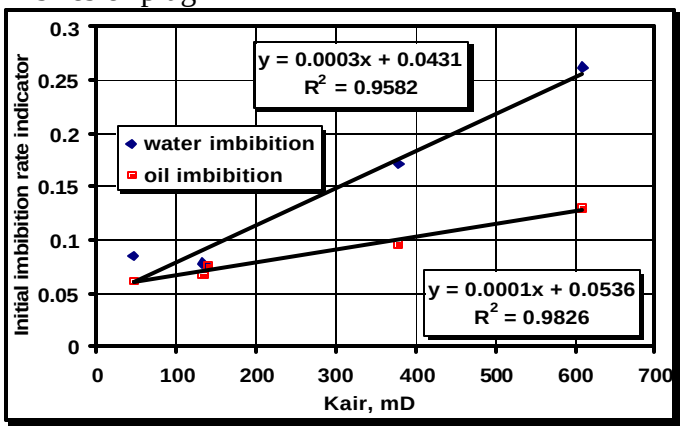

Figure 15: Initial imbibition rate indicator as a function of air permeability

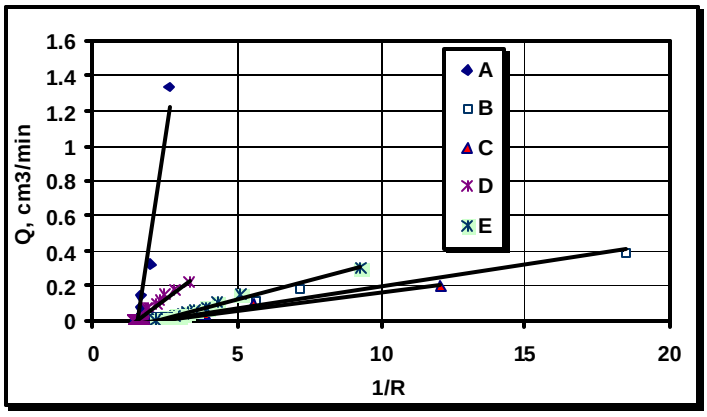

Figure 16: Water imbibed rate as the function of reciprocal of gas recovery

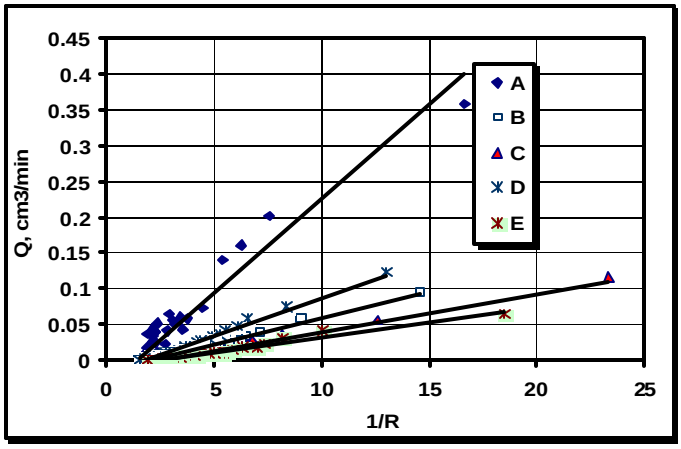

Figure 17: Oil imbibed rate as the function of reciprocal of gas recovery

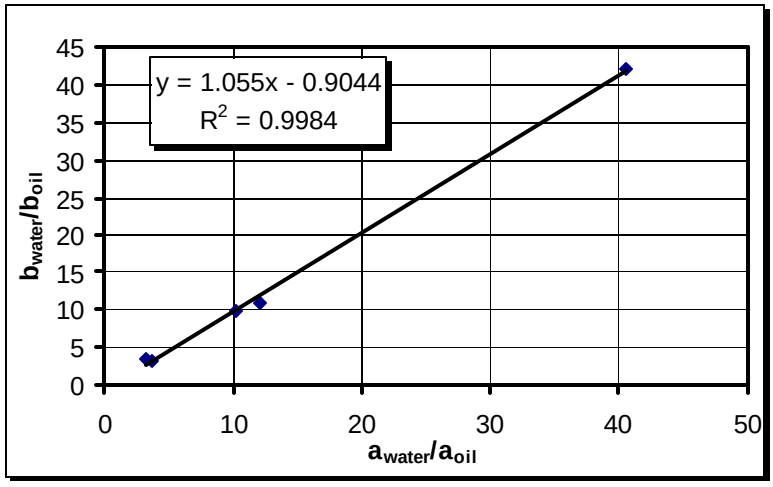

Figure 18: Correlation of coefficient between oil and water imbibition tests